Formation of Single-Crystal-like Poly(9,9-dioctylfluorene) Thin Film by the Friction-Transfer Technique with Subsequent Thermal Treatments

Masahiro Misaki,[†] Yasukiyo Ueda,*[,†] Shuichi Nagamatsu,[‡] Yuji Yoshida,[‡] Nobutaka Tanigaki,[‡] and Kiyoshi Yase[‡]

Graduate School of Science and Technology, Kobe University, 1-1 Rokko, Nada, Kobe 657-8501, Japan, and Photonics Research Institute, National Institute of Advanced Industrial Science and Technology (AIST), Tsukuba Central 5, 1-1-1 Higashi, Tsukuba 305-8565, Japan

Received May 14, 2004; Revised Manuscript Received July 1, 2004

ABSTRACT: A liquid-crystalline polymer, poly(9,9-dioctylfluorene) (PFO), was found to form highly oriented films by a friction-transfer technique. The polarized UV−vis absorption and photoluminescence spectra of the films formed showed strong dichroism with a dichroic ratio of approximately 10 in the drawing direction of friction transfer. Subsequent thermal treatments of the friction-transferred PFO films were specifically effective for the improvement of the physical properties, structure, and morphology of the films. By rapid and slow cooling from the liquid-crystalline melted states of the friction-transferred films, liquid-crystalline and crystalline films were prepared, respectively. Both thermally treated films showed enhanced optical anisotropy with a dichroic ratio of approximately 25 in photoluminescence spectra. The electron diffraction pattern of the crystalline film showed a large number of sharp diffraction spots as seen in a single crystal. The liquid-crystalline polymer was found to form a single-crystal-like thin film by the friction-transfer technique with subsequent thermal treatments.

Introduction

Conjugated polymers have aroused interest for various applications such as field-effect transistors (FETs),[1] photovoltaic cells,[2] and light-emitting diodes (LEDs)[3] due to their excellent electrical and optical properties, reasonable chemical stability, and ease of processability. Also, conjugated polymers are expected to exhibit anisotropic properties because the intrinsic characteristic of conjugated polymers originates from the electrons delocalized along the polymer backbone (main chain).[4−8] Therefore, the arrangement of conjugated polymers is very important for their physical properties in films. However, films prepared without using a polymer arrangement technique exhibit isotropic properties. Various methods such as the Langmuir−Blodgett (LB) technique,[9,10] stretching[11,12] or rubbing of the conjugated polymer,[13] and the deposition of the latter onto an alignment layer[14] have been applied to the arrangement of polymers.

There are various benefits of using oriented films in electronic devices. For instance, oriented films result in an emission of linearly polarized light when used in LEDs[15,16] and in an enhanced mobility when used in FETs.[7] For fabricating such devices using a liquid-crystalline (LC) polymer, the alignment layer, such as rubbed polyimide, is commonly positioned between the electrode and an active semiconducting layer. The problem in this method is that the intermediate alignment layer is generally an electrical insulator, leading to poor device performance. Several attempts to remove the intermediate alignment layer from oriented films have been made.[17−19]

One of the powerful methods of arranging the polymer backbone is the friction-transfer technique. When polymers, such as poly(tetrafluoroethylene) (PTFE), are squeezed and drawn against a clean surface of metal or glass, a very thin film of the polymer remains at the surface.[20] Highly oriented polymer backbones were observed along the drawing direction by transmission electron microscopy[21,22] and X-ray diffraction analysis.[23] Moreover, Wittmann and Smith reported that a friction-transferred PTFE film can be used to orient other materials.[21] By using the friction-transfer technique, polymers can be arranged without using an intermediate alignment layer. We have applied this technique to the preparation of films of conjugated polymers, such as polysilane (PS), poly(*p*-phenylene) (PPP), poly(*p*-phenylenevinylene) (PPV), poly(alkylthiophene)s (PAT), and their derivatives.[24−28] Also, we demonstrated that such films have a large optical anisotropy and in-plane anisotropic physical properties.[29−31]

Scheme 1. Structure of PFO

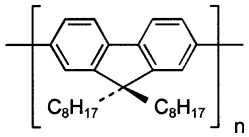

In the present study, we apply the friction-transfer technique to the preparation of highly oriented films of LC polymer, poly(9,9-dioctylfluorene) (PFO) (see Scheme 1). PFO has emerged as an attractive material for LEDs,[32,33] owing to its efficient blue emission and high hole mobility greater than 3×10^{-4} cm^2/(V s).[34] PFO exhibits thermal liquid crystallinity, leading to the alignment of PFO when annealed on a rubbed substrate.[35] Therefore, we investigate the effects of thermal treatment on the spectroscopic properties, structure, and morphology of friction-transferred films. Here we report that a single-crystal-like PFO thin film was successfully achieved by the friction-transferred technique with subsequent thermal treatments without using an intermediate alignment layer.

* Corresponding author: e-mail yueda@kobe-u.ac.jp.
[†] Kobe University.
[‡] AIST.

10.1021/ma049051x CCC: $27.50
Published on Web 08/10/2004

Experimental Section

PFO was used as purchased (American Dye Source, Inc.). The typical polystyrene equivalent number- and weight-average molecular weights, as determined by gel permeation chromatography (GPC, Shimadzu LC-10Vp HPLC System) with a TOSOH G5000H_{HR} GPC column calibrated using a polystyrene standard, are M_n = 25 000 and M_w = 55 000 (polydispersity = 2.2), respectively. The differential scanning calorimetry (DSC, Perkin-Elmer Instruments) scans showed a crystallization peak at approximately 80−90 °C and a melting endothermal peak at approximately 160 °C at a heating/cooling rate of 20 °C/min. Above this temperature, PFO shows birefringent LC melt and becomes isotropic at approximately 270−280 °C.[35]

PFO films were prepared on quartz substrates by the friction-transfer technique. PFO powder was compressed into a pellet. The friction-transfer process was carried out in a nitrogen atmosphere by squeezing and drawing the pellet on the substrate kept at a controlled temperature. The applied load for squeezing was 3 kgf/cm^2, and the drawing speed was 0.3 m/min. The thickness of the resulting films was determined by a surface profile tracer (TENCOR Instruments).

For the improvement of molecular alignments in the films, the friction-transferred PFO films were then treated by two different thermal procedures according to the literature.[35] In one case, the PFO films were heated at 200 °C for 1 h and then rapidly cooled to room temperature. In the other case, the PFO films were heated at 200 °C and then slowly cooled to room temperature at a rate of 0.2 °C/min. All procedures were carried out in a nitrogen atmosphere to prevent thermal oxidation. Note that, in our experiments, the PFO films were thermal-treated without an intermediate arrangement layer. We call a friction-transferred film, a rapidly cooled film, and a slowly cooled film the "as-deposited film", "LC film", and "crystalline film", respectively.

For optical measurements, the films were characterized using an ultraviolet−visible (UV−vis) absorption spectrometer (Shimadzu MPS2000) and a fluorescence spectrometer (JASCO FP777). In these optical measurements, a Glan-Tomson prism was used to characterize dichroism in the films. Dichroic ratio in absorption can be defined as the ratio of $A_{\parallel}$ to $A_{\perp}$, where $A_{\parallel}$ and $A_{\perp}$ are the polarized absorptions parallel and perpendicular to the drawing direction of friction transfer, respectively. Also, the dichroic ratio in photoluminescence (PL) can be defined as the ratio of $I_{\parallel}$ to $I_{\perp}$, where $I_{\parallel}$ and $I_{\perp}$ are the polarized emissions parallel and perpendicular to the drawing direction of friction transfer, respectively. (Nonpolarized light was used as excited light.) These dichroic ratios reflect the degree of alignment in the films.

For morphological and structural analyses, the films were observed by atomic force microscopy (AFM, Seiko Instruments Inc., Nanopics NPX100M001) and transmission electron microscopy (TEM, HITACHI H-7100). For TEM observation, after the specimen PFO films were reinforced with evaporated carbon, the films on the substrate were exposed to hydrofluoric acid for a few minutes and separated from the substrate by dipping in water. The specimen PFO films were transferred onto a microgrid. The transmission electron micrographs and the electron diffraction patterns were recorded at an acceleration voltage of 100 kV.

Results and Discussion

1. Film Preparation by the Friction-Transfer Technique. The quality of the friction-transferred film strongly depended on substrate temperature. PFO was not transferred onto the substrate at a substrate temperature below 60 °C. The PFO transferred at a substrate temperature between 60 and 70 °C formed a powdery film, whereas the PFO transferred at a substrate temperature between 80 and 110 °C formed uniform film. We decided that the optimum temperature for transfer was approximately 90 °C on the basis of the dichroic ratio (discussed below). The thickness of the film prepared at 90 °C was approximately 50 nm.

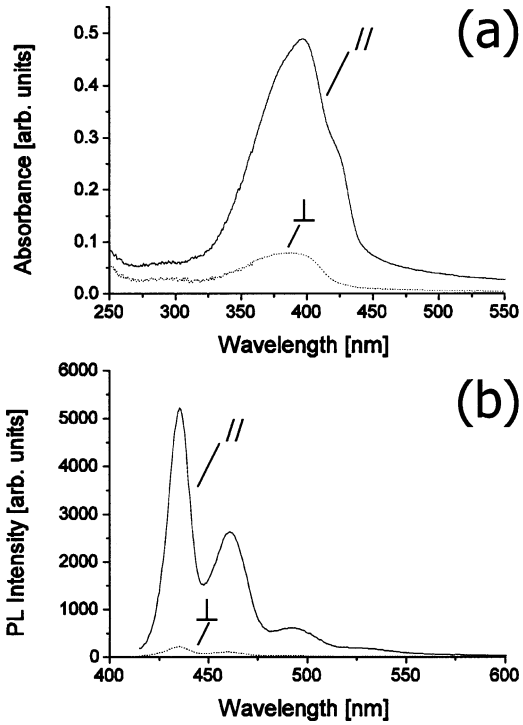

Figure 1. (a) Polarized UV−vis absorption and (b) PL spectra of friction-transferred PFO film. In each case, the polarization direction is parallel (solid line) or perpendicular (dashed line) to the drawing direction. For PL spectra, the excitation wavelength was 390 nm.

The molecular arrangements, the polymer backbone in particular, in the films were evaluated by polarized optical spectroscopy. Figure 1a shows the polarized UV−vis absorption spectra of the film prepared at 90 °C. The absorption spectra showed different profiles depending on the type of polarization. In the parallel polarization, a major absorption maximum was observed at 397 nm with a shoulder in the long-wavelength edge of the band, which was associated with delocalized $\pi-\pi^*$ transitions on fluorene backbones. In the perpendicular polarization, however, this peak was sufficiently suppressed. Thus, the film exhibited a strong dichroism with a dichroic ratio at an absorption maximum of approximately 7, which indicates that polymer backbones in the film were highly aligned parallel to the drawing direction.

Figure 1b shows the polarized PL spectra of same sample. The PL spectrum with the parallel polarization showed a well-resolved vibronic progression with peaks at 435, 460, and 493 nm. On the other hand, these peaks were sufficiently suppressed in the PL spectrum with the perpendicular polarization. The dichroic ratio in PL was approximately 10 for the peak at 435 nm. We assumed that the higher dichroism in PL than in absorption might be consistent with the migration of excitons to the lowest energy, most highly oriented segments of the polymer before emission occurred.[16]

The alignment of PFO has first been demonstrated on rubbed polyimide by Grell el al.[35] They reported that the dichroic ratios in absorption and PL are approximately 6.5 and 10, respectively.[15,16,35] Our results of the dichroic ratios for the friction-transferred films were almost comparable to those for molecular arrangements on rubbed polyimide. We note that the friction-transfer

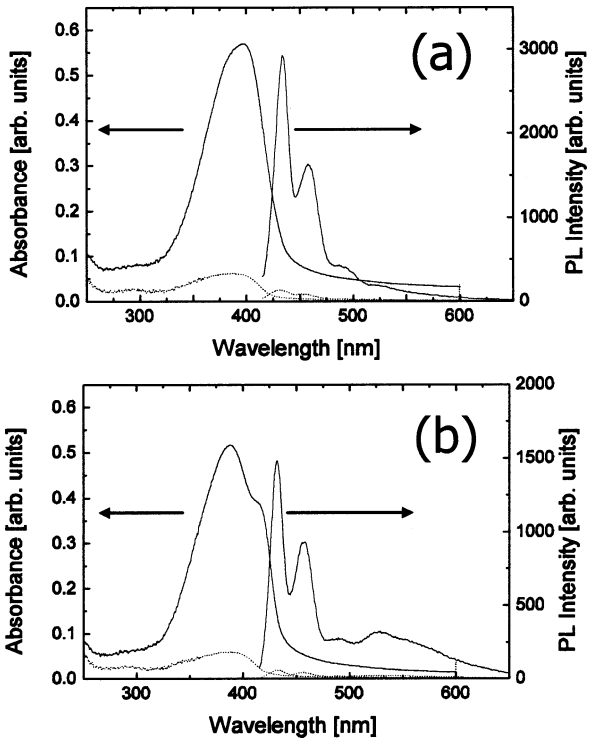

Figure 2. Polarized UV−vis absorption and PL spectra of (a) LC film and (b) crystalline film. In each case, the polarization direction is parallel (solid line) or perpendicular (dashed line) to the drawing direction. For PL spectra, the excitation wavelength was 390 nm.

technique is a very simple but powerful method of arranging a polymer backbone without using an intermediate alignment layer.

2. Effect of Thermal Treatments. 2.1. Spectroscopic Properties. One interesting feature observed in PFO is the appearance of thermotropic liquid crystallinity, leading to the alignment of PFO when annealed on rubbed polyimide.[35] We are interested in the effects of thermal treatments on the properties and structures of friction-transferred PFO film, which does not have an intermediate alignment layer. All procedures for the thermal treatments have been described in the Experimental Section.

Figure 2 shows the results of polarized UV−vis absorption and PL spectra of (a) the LC film and (b) crystalline film. In both thermal treatments, the dichroic ratios in absorption and PL were approximately 10 and 25, respectively, indicating an excellent uniaxial alignment of the polymer backbone. Such high dichroic ratios, particularly in PL, have not yet been reported in PFO films prepared by other polymer backbone alignment methods.

We note that the degree of alignment in the as-deposited film was improved by subsequent thermal treatments without using an intermediate alignment layer. In the case of LC alignment on rubbed polyimide, the ordered polyimide chains induce a preferred molecular alignment in the adsorbed LC monolayer, and then the orientation of the first LC monolayer can effectively determine homogeneous bulk alignment.[36,37] We assume that a similar mechanism can cause the rearrangement in the LC melted states of the friction-transferred film. It is considered that the friction-transferred polymer chains at the interface between a polymer and a substrate may be firmly fixed to the substrate even at the melting temperature. Tanigaki et al. have reported that a melted friction-transferred PTFE film recrystallizes into the same polymer arrangement as that of an as-deposited PTFE film.[23] This result indicates that the orientation of whole polymer chains in films can be controlled by immobilized polymer chains at the interface. However, it has never been reported that the degree of alignment in friction-transferred films is improved by subsequent thermal treatments.

From these viewpoints, we consider the rearrangement mechanism of thermally treated films as follows. First, polymer chains at the nearest interface of the substrate are highly ordered and firmly fixed to the substrate by the friction-transfer technique. Second, the orientation of the immobilized polymer chains at the interface induces the homogeneous bulk alignment above the LC transition temperature. Finally, the rearrangement of whole polymer chains in the films is achieved when the films are cooled to room temperature. Thus, we conclude that dichroic ratio increases with subsequent thermal treatments because disordered polymer chains in the as-deposited film are realigned along the drawing direction.

There are some differences in optical properties between the LC and crystalline films depending on the different thermal treatments. The LC film showed a relatively narrow peak at 397 nm in absorption and a clear vibronic structure with peaks at 434, 458, and 487 nm in PL for the parallel polarization. On the other hand, the crystalline film showed a peak at 388 nm with a shoulder in the long-wavelength edge of the band in absorption and a clear vibronic structure with peaks at 432, 458, and 490 nm with a broad structureless green emission at approximately 530 nm in PL for the parallel polarization. It is assumed that the differences in optical spectra between the LC and crystalline films result from the difference in structure between the films (discussed below).

2.2. Film Structure and Morphology. According to the results of the optical measurements, both the LC and crystalline films showed an excellent uniaxial alignment of the polymer backbone, but there were some differences in optical spectra between them. To obtain structural information on each PFO film, we carried out TEM observation. The transmission electron micrographs and electron diffraction patterns are shown in Figure 3. Note that the drawing direction (fiber axis) is always vertical. These data showed a considerable difference in polymer arrangement between the films.

Figure 3a,b shows a transmission electron micrograph and an electron diffraction pattern of the as-deposited film. The transmission electron micrograph showed long grains with a preferred orientation parallel to the drawing direction. The electron diffraction pattern displayed a fiber pattern with several diffraction arcs, indicating an in-plane uniaxial orientation. One interesting feature shown in Figure 3b is the appearance of strong diffraction arcs along the meridian with an interplanar spacing of 0.42 nm, which is same as that observed in grazing-incidence X-ray diffraction (GIXRD) studies using synchrotron radiation on PFO thin films by Kawana et al. and can be identified as the benzene ring repeat distance along the polymer backbone (0.42 nm).[38] This benzene periodic distance is half the fluorene monomer periodic distance. On the other hand, there are a series of diffraction arcs with a repeat distance of 1.17 nm perpendicular to the fiber axis. It is considered that this periodicity is governed by the

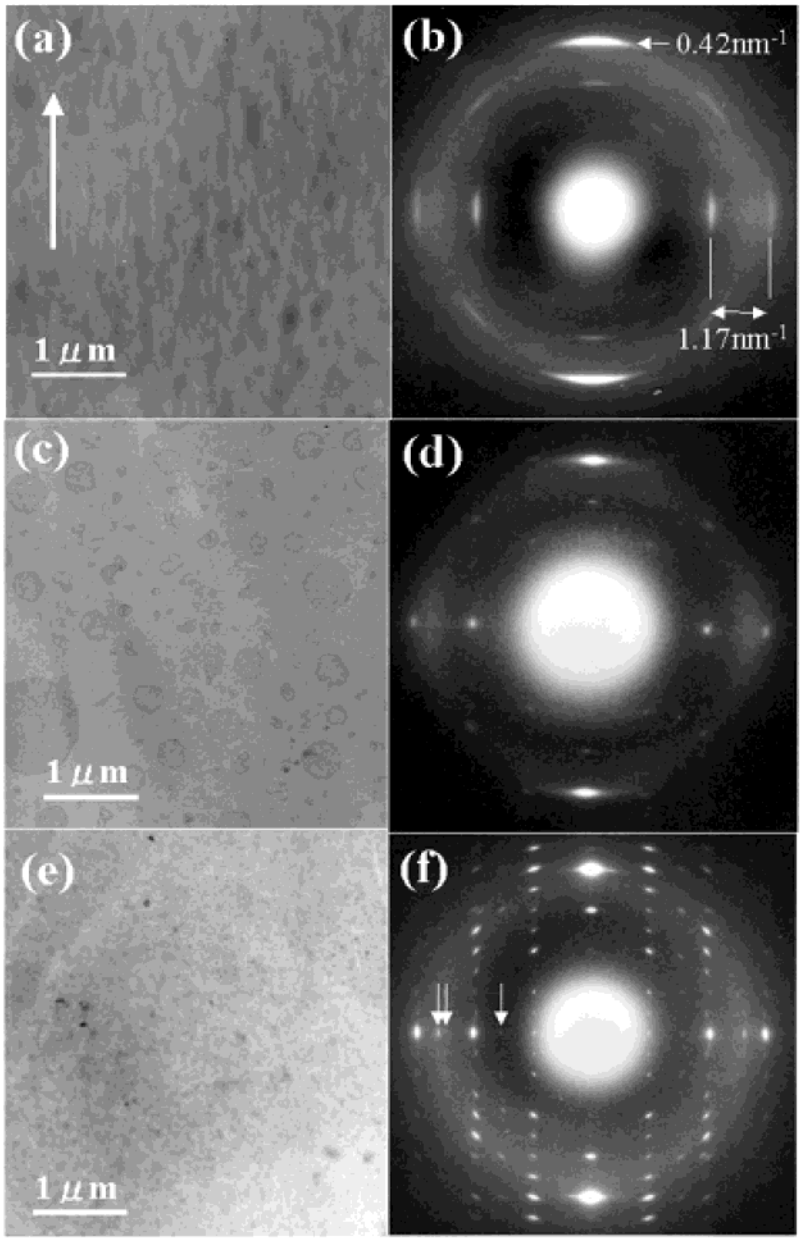

Figure 3. Transmission electron micrographs and electron diffraction patterns of (a, b) as-deposited film, (c, d) LC film, and (e, f) crystalline film. The arrow indicates the drawing direction.

alkyl side-chain length (1 nm). Therefore, we conclude that the polymer backbone lies in the film along the drawing direction and forms periodic side packs with the spacing governed by the alkyl side-chain length.

Figure 3c,d shows a transmission electron micrograph and an electron diffraction pattern of the LC film. In the transmission electron micrograph (Figure 3c), two types of growth habit were observed. One is the part of spherical crystals of submicrometer diameter, and the other is the part of featureless uniform morphology. Although the electron diffraction pattern in Figure 3d shows an almost pattern similar to that in Figure 3b, it shows no arcs but only sharp spots. This indicates that the degree of polymer arrangement in the glassy film was higher than that in the as-deposited film. Figure 3d also shows diffused scattering in both the equator and meridian, which is typical of a nematic crystal with its director pointing along the fiber axis. Therefore, we conclude that the LC film is composed of a mixture of LC glass and crystalline fractions. In both parts, because the molecular axis is parallel to the drawing direction, the observed large dichroism in polarized optical spectra can be explained. We note that the ratio of growth habits between LC glass and crystalline fractions may strongly depend on the speed of quenching to room temperature.

Figure 3e,f shows a transmission electron micrograph and an electron diffraction pattern of the crystalline film. The transmission electron micrograph showed no significant texture, indicating a homogeneous morphology of the crystalline film. The diffraction pattern of the crystalline film showed a large number of sharp diffraction spots. Again, strong diffraction spots were observed at a spacing of 0.42 nm along the meridian and a repeat distance of 1.17 nm along the equator, which can be identified as the benzene ring repeat distance along the polymer backbone and the side-packing distance governed by the alkyl side-chain length, respectively. The structure resembles that observed in aligned fibers after physicochemical treat-

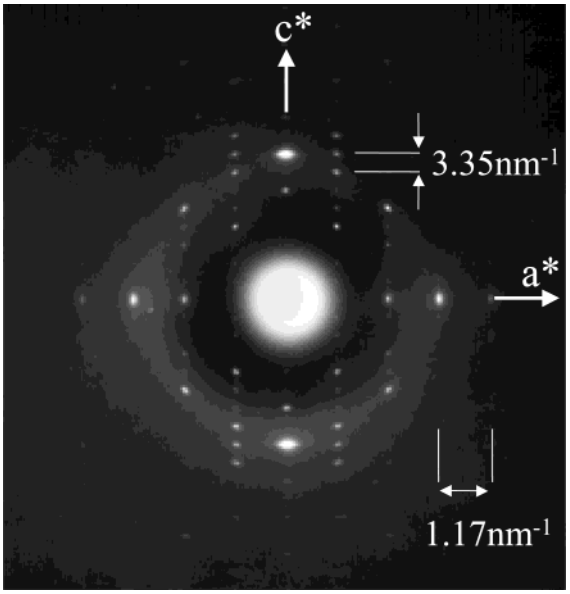

Figure 4. Microelectron diffraction pattern of crystalline film.

ments, which is characterized by a fiber repeat of 3.35 nm along the fiber axis, equal to four monomer units.[39] Figure 3f also shows additional weak diffraction spots corresponding to spacings of 0.77, 0.47, and 0.45 nm in the equator (indicated by arrows). We believe that these weak diffraction spots arise from a distortion of the sample rather than from different orientations.

Figure 4 shows a selected area electron diffraction pattern from a circular area of 5 μm diameter in the crystalline film. The electron diffraction pattern displayed a single net pattern with the diffraction spots corresponding to the interplanar distances of 3.35 and 1.17 nm, suggesting that PFO molecules are arranged as a single crystal on the microscopic scale. This is the first observation of the single-crystal-like arrangement in the PFO thin film. The two-dimensional crystal parameters of PFO are determined to be $a = 1.17$ nm and $c = 3.35$ nm (fiber axis). Therefore, we conclude that improved intra- and interchain registries in the crystalline film may give rise to the spectrum with a shoulder in absorption and the green emission in PL. Further experiments are being planned to analyze three-dimensional structures in the films by energy-dispersion total-reflection X-ray diffraction (ED-TRXD) analysis for the measurement of whole reciprocal lattice spaces,[23] and the results will be reported separately.

The surface morphologies of PFO films were investigated by AFM. Figure 5a shows the as-deposited film surface morphology, revealing a rough topography with height variations of approximately 40 nm. On the other hand, Figure 5b shows the LC film surface, revealing a smooth topography with height variations of approximately 5 nm. The same smooth topography as the LC film surface was observed in the crystalline film. Thus, the surface morphology of the as-deposited film was drastically smoothened by subsequent thermal treatments. A smooth topography is advantageous to device applications such as in LEDs and FETs.

Conclusions

The highest degree of alignment in PFO films was achieved by the friction-transfer technique with subsequent thermal treatments. Both the LC and crystalline films showed enhanced optical anisotropy, indicating an excellent uniaxial alignments of polymer backbones parallel to the drawing direction. However, each thermally treated film had different film structures and morphologies. The LC film showed a mixed structure of both the LC glass and crystalline fractions, while the crystalline film showed a single-crystal-like structure. The two-dimensional crystal parameters of PFO are determined to be $a = 1.17$ nm and $c = 3.35$ nm (fiber axis).

The surface morphology of the as-deposited film was improved by subsequent thermal treatments, which is advantageous to device applications. Since physical properties are also affected by molecular arrangement, an active semiconducting layer with an intrinsic in-plane anisotropy can be prepared by the friction-transfer technique. For instance, when LEDs are prepared using an aligned polymer as an emission layer, they emit polarized light,[30] and when FETs are prepared using an aligned polymer as a semiconducting layer, they show a large in-plane anisotropy of carrier mobility.[29] The fabrication of some new devices with highly anisotropic physical properties using the friction-transfer technique is currently under way.

Acknowledgment. The authors thank Dr. T. Kimura for GPC and DSC measurements and Dr. M. Chikamatsu and Dr. T. Taima (AIST) for helpful discussions.

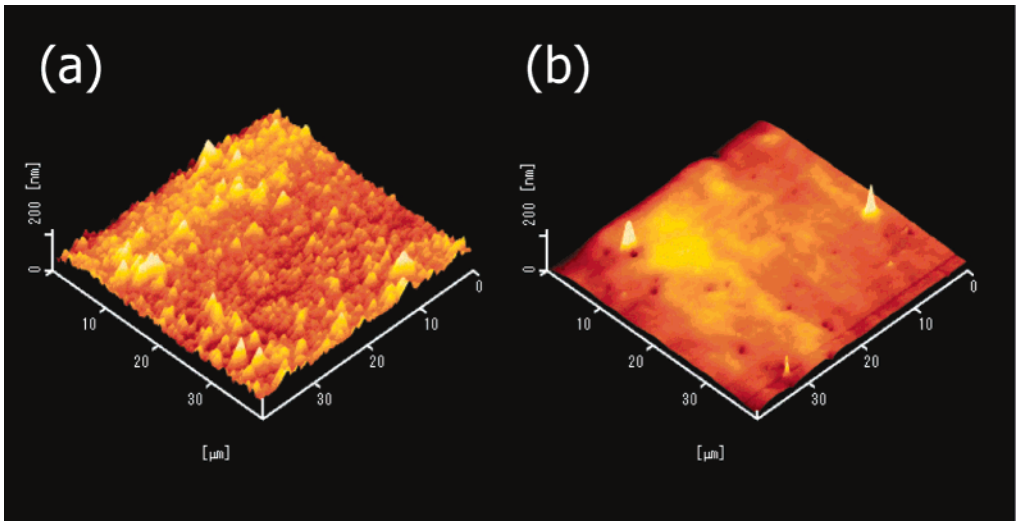

Figure 5. AFM images of (a) as-deposited film and (b) LC film.

We are grateful to Dr. M. Yamashita (Tokyo University of Science) for AFM measurements.

References and Notes

(1) Tsumura, A.; Koezuka, H.; Ando, T. *Appl. Phys. Lett.* **1986**, *49*, 1210.
(2) Brabec, C. J.; Sariciftci, N. S.; Hummelen, J. C. *Adv. Funct. Mater.* **2001**, *11*, 15.
(3) Friend, R. H.; Gymer, R. W.; Holmes, A. B.; Burroughes, J. H.; Marks, R. N.; Taliani, C.; Bradley, D. D. C.; Dos Santos, D. A.; Brédas, J. L.; Lögdlund, M.; Salaneck, W. R. *Nature (London)* **1999**, *397*, 121.
(4) Sirringhaus, H.; Brown, P. J.; Friend, R. H.; Nielsen, M. M.; Bechgaard, K.; Langeveld-Van, B. M. W.; Spiering, A. J. H.; Janssen, R. A. J.; Meijer, E. W.; Herwing, P.; de-Leeuw, D. M. *Nature (London)* **1999**, *401*, 685.
(5) Aasmundtveit, K. E.; Samuelsen, E. J.; Guldstein, M.; Steinsland, C.; Flornes, O.; Fagermo, C.; Seeberg, T. M.; Pettersson, L. A. A.; Inganäs, O.; Feidenhans'l, R.; Ferrer, S. *Macromolecules* **2000**, *33*, 3210.
(6) Xu, G.; Bao, Z.; Groves, J. T. *Langmuir* **2000**, *16*, 1834.
(7) Sirringhaus, H.; Wilson, R. J.; Friend, R. H.; Inbasekaran, M.; Wu, W. W.; Woo, E. P.; Grell, M.; Bradley, D. D. C. *Appl. Phys. Lett.* **2000**, *77*, 406.
(8) Amundson, K. R.; Sapjeta, B. J.; Lovinger, A. J.; Bao, Z. *Thin Solid Films* **2002**, *414*, 143.
(9) Cimrova, V.; Remmers, M.; Neher, D.; Wegner, G. *Adv. Mater.* **1996**, *8*, 146.
(10) Bolognesi, A.; Bajo, G.; Paloheimo, J.; Östergard, T.; Stubb, H. *Adv. Mater.* **1997**, *9*, 121.
(11) Dyreklev, P.; Berggren, M.; Inganäs, O.; Andersson, M. R.; Wennerström, O.; Hjertberg, T. *Adv. Mater.* **1995**, *7*, 43.
(12) Lemmer, U.; Vacar, D.; Moses, D.; Heeger, A. J.; Ohnishi, T.; Noguchi, T. *Appl. Phys. Lett.* **1996**, *68*, 3007.
(13) Hamaguchi, M.; Yoshino, K. *Appl. Phys. Lett.* **1995**, *67*, 3381.
(14) Lüssem, G.; Geffarth, F.; Greiner, A.; Heitz, W.; Hopmeier, M.; Oberski, M.; Unterlechner, C.; Wendorff, J. H. *Liq. Cryst.* **1996**, *21*, 903.
(15) Grell, M.; Bradley, D. D. C. *Adv. Mater.* **1999**, *11*, 895.
(16) Whitehead, K. S.; Grell, M.; Bradley, D. D. C.; Jandke, M.; Strohriegl, P. *Appl. Phys. Lett.* **2000**, *76*, 2946.
(17) Jandke, M.; Strohriegl, P.; Gmeiner, J.; Brütting, W.; Schwoerer, M. *Adv. Mater.* **1999**, *11*, 1518.
(18) Bolognesi, A.; Botta, C.; Facchinetti, D.; Jandke, M.; Kreger, K.; Strohriegl, P.; Relini, A.; Rolandi, R.; Blumstengel, S. *Adv. Mater.* **2001**, *13*, 1072.
(19) Godbert, N.; Burn, P. L.; Gilmour, S.; Markham, J. P. J.; Samuel, I. D. W. *Appl. Phys. Lett.* **2003**, *83*, 5347.
(20) Makinson, K. R.; Tabor, D. *Proc. R. Soc. London* **1964**, *A281*, 49.
(21) Wittmann, J. C.; Smith, P. *Nature (London)* **1991**, *352*, 414.
(22) Ueda, Y.; Kuriyama, T.; Hari, T.; Ashida, M. *J. Electron Microsc.* **1994**, *43*, 99.
(23) Tanigaki, N.; Yoshida, Y.; Kaito, A.; Yase, K. *J. Polym. Sci., Part B: Polym. Phys.* **2001**, *39*, 432.
(24) Tanigaki, N.; Kyotani, H.; Wada, M.; Kaito, A.; Yoshida, Y.; Han, E. M.; Abe, K.; Yase, K. *Thin Solid Films* **1998**, *331*, 229.
(25) Tanigaki, N.; Yase, K.; Kaito, A.; Ueno, K. *Polymer* **1995**, *36*, 2477.
(26) Tanigaki, N.; Yase, K.; Kaito, A. *Mol. Cryst. Liq. Cryst.* **1995**, *267*, 335.
(27) Yoshida, Y.; Tanigaki, N.; Yase, K.; Hotta, S. *Adv. Mater.* **2000**, *12*, 1587.
(28) Nagamatsu, S.; Takashima, W.; Kaneto, K.; Yoshida, Y.; Tanigaki, N.; Yase, K. *Macromolecules* **2003**, *36*, 5252.
(29) Nagamatsu, S.; Takashima, W.; Kaneto, K.; Yoshida, Y.; Tanigaki, N.; Yase, K. *Appl. Phys. Lett.* **2004**, *84*, 4608.
(30) Yoshida, Y.; Ni, J. P.; Tanigaki, N.; Yase, K. *Mol. Cryst. Liq. Cryst.* **2001**, *370*, 69.
(31) Tanigaki, N.; Kuwajima, S.; Nagamatsu, S.; Yoshida, Y.; Yase, K. *Synth. Met.* **2003**, *137*, 1425.
(32) Grice, A. W.; Bradley, D. D. C.; Bernius, M. T.; Inbasekaran, M.; Wu, W. W.; Woo, E. P. *Appl. Phys. Lett.* **1998**, *73*, 629.
(33) Neher, D. *Macromol. Rapid Commun.* **2001**, *22*, 1365.
(34) Redecker, M.; Bradley, D. D. C.; Inbasekaran, M.; Woo, E. P. *Appl. Phys. Lett.* **1998**, *73*, 1565.
(35) Grell, M.; Bradley, D. D. C.; Inbasekaran, M.; Woo, E. P. *Adv. Mater.* **1997**, *9*, 798.
(36) Zhuang, X.; Marrucci, L.; Shen, Y. R. *Phys. Rev. Lett.* **1994**, *73*, 1513.
(37) Kim, D.; Oh-e, M.; Shen, Y. R. *Macromolecules* **2001**, *34*, 9125.
(38) Kawana, S.; Durrell, M.; Lu, J.; Macdonald, J. E.; Grell, M.; Bradley, D. D. C.; Jukes, P. C.; Jones, R. A. L.; Bennett, S. L. *Polymer* **2002**, *43*, 1907.
(39) Grell, M.; Bradley, D. D. C.; Ungar, G.; Hill, J.; Whitehead, K. S. *Macromolecules* **1999**, *32*, 5810.

MA049051X